



# Seismic performance detection by fragility analysis: a comparison between standard and alternative approaches

Matteo Ciano<sup>a</sup>, Massimiliano Gioffrè<sup>a</sup>, Mircea Grigoriu<sup>b</sup>

<sup>a</sup>Dept. of Civil and Environmental Engineering, Univ. of Perugia, Via G. Duranti 93, 06125 Perugia, Italy

<sup>b</sup>Dept. of Civil and Environmental Engineering, Cornell Univ., Ithaca, NY 14853, USA

*Keywords: Seismic intensity measures; Fragility curves; Fragility surfaces; Activity matrix; Earthquake engineering; Complex mdof structural system;*

## ABSTRACT

Performance-based design rely on evaluating structural efficiency by fragilities. Seismic fragilities are the probability that the structural response of a system overcomes specified limit states for given seismic intensity measure. Usually these curves are obtained by scaling seismic accelerograms by a reference intensity measure (e.g. single/multiple ordinates of the pseudo-acceleration response spectrum or peak ground acceleration). This approach, together with Monte Carlo simulation, overcomes the problem of the limited number of natural recorded ground motions available for fragility analysis, but it is not accurate to describe the probability law of the original unscaled records. Furthermore, if the dependence between the intensity measure and various system demand parameters (e.g. max inter-story displacement) is weak the fragility with these intensity measures provides limited if any information on the structural seismic performance. The aim of this paper is to estimate fragilities using standard and alternative approaches for a complex multi-degree of freedom structural system. In the alternative approach the seismic inputs to the system are described through the site seismic activity matrix. An actual multi-degree of freedom structural system is considered as a case study. In particular, a school building in Norcia is used to show standard and alternative approaches in fragilities estimation.

## 1 INTRODUCTION

Seismic fragilities are the probability that the structural response of a system overcomes specified limit values for given seismic intensity measures (*IMs*). Performance-Based Earthquake Engineering (PBEE) ambition is to evaluate structural efficiency by fragility analysis. The Federal Emergency Management Agency (FEMA) recommends to estimate the seismic fragility curve by a standard approach based on scaling the seismic accelerograms with a reference intensity measure *IM* (FEMA P-58 2012a). Commonly the incremental dynamic analysis (IDA) is used to develop fragility analysis. The IDA yields a distribution of results at varying intensities that can be used to generate a collapse fragility (FEMA P-58 2012a). This approach, together with Monte Carlo simulation, overcomes the problem of the limited number of

natural recorded ground motions available for fragility analysis.

Two groups of *IMs* are usually used to define the seismic fragilities: (i) functional of samples of seismic ground acceleration process  $A(t)$ , such as peak ground acceleration (PGA); (ii) functional of filtered version of samples of  $A(t)$ , e.g. single/multiple ordinates of pseudo-acceleration response spectrum  $S_a(T)$  for different structural system periods  $T$  (Lopez Garcia and Soong 2003; O'connor and Ellingwood 1992). In particular, the *IMs* in the second group, that are widely used to define the fragilities, depend on the kind of system demand parameter  $D$  (e.g. max inter-story displacement) on which the analysis is based (Ebrahimian et al. 2015; Kwong et al. 2015a, 2015b, 2015c).

The usefulness of standard procedures based on scaled seismic ground motion acceleration is indisputable, but it was shown not to be accurate when describing the probability law of the

original unscaled records (Grigoriu 2010). Fragilities based on scaled ground motions provide limited information on the seismic performance of structural systems. Moreover, the dependence between the  $D$  and  $IM$  plays a fundamental role in the fragilities estimation (Grigoriu 2016). If they are independent, the obtained fragility can provide limited information on the performance of the structural system. One of these Authors (Grigoriu 2016) showed that the fragilities defined as function of  $S_a(T)$  for nonlinear single degree of freedom (SDOF) system to seismic acceleration process  $A(t)$  have large uncertainties when  $D$  and  $S_a(T)$  are weakly correlated. Furthermore, the fragilities defined as function of multiple ordinates of  $S_a(T)$  have poor improvements in reference to the case of single ordinate of  $S_a(T)$ . It was demonstrated that the dependence between IMs and various system demand parameters,  $D$ , is weak for nonlinear system and also for complex multi-degree of freedom (MDOF) linear structures (Ciano et al. submitted; 2018; Grigoriu 2016).

The aim of this work is to estimate fragilities by an alternative approach as proposed in (Kafali and Grigoriu 2007; Radu 2017; Radu and Grigoriu 2018) for a complex multi-degree of freedom structural system and to compare the results to those obtained by the standard approach. In the alternative approach the process  $A(t)$  is defined starting from the site seismic activity matrix (SAM), in order to define samples of the seismic acceleration process  $A(t)$  by an alternative  $IM$  based on two parameters (e.g. vector-valued  $IM$ ): the earthquake moment magnitude  $m$  and the distance  $r$  from the seismic source to system site. The SAM, for selected site, provides, for each couple  $(m, r)$ , the earthquake probability of occurrence. An actual multi-degree of freedom structural system, a school building in Norcia, Italy, is considered as case study. This construction is equipped with nonlinear dissipative steel bracing, and its numerical model is calibrated using experimental data obtained by the Italian National Seismic Observatory.

Finally, the results of the fragilities obtained by the two approaches is shown. Different scalar  $IMs$  are used to estimate fragilities by the standard method and the influence of the dependence between  $D$  and  $IM$  on these curves are shown. It is remarked that the estimation of fragility curves by the procedure based on SAM

can provide information on the seismic performance of the structural system.

## 2 BACKGROUND

### 2.1 Problem definition

Let  $I$  be the set of demand parameters which yield a structural failure. The fragility can be defined as

$$P_f(\xi) = P(D \in I \subset \mathfrak{R} \mid IM = \xi) \\ = E[1(D \in I \mid IM = \xi)] = \int_I f_{D|IM}(x \mid \xi) dx \quad (1)$$

i.e. the probability that a structural system enters a damage state given a ground motion with scalar/vector intensity measure  $IM=\xi$ . The quantities  $1(\cdot)$  and  $f_{D|IM}(\cdot|\xi)$  indicate the indicator function and probability density function (PDF) of the conditional variable  $D|(IM=\xi)$ , respectively. The fragility in (1) is usually estimated from the structural response to scaled seismic time histories,  $a(t)$  of the stochastic process  $A(t)$  (Baker 2010), and its accuracy depends on the scaling procedure, the sample size and the  $IMs$  properties.

When  $D$  and  $IM$  are strongly dependent, the random variable  $D/IM$  has small variance, i.e.  $f_{D/IM}(\cdot|\xi)$  is concentrated about its mean value. On the contrary, when  $D$  and  $IM$  are weakly dependent the random variable  $D/IM$  has large variance. In the limit,  $f_{D/IM}(\cdot|\xi)$  becomes a  $\delta$ -function or  $D$  and  $D/IM$  have the same PDF when  $D$  and  $D/IM$  are perfectly correlated or independent, respectively (Grigoriu 2016). In the latter case, the fragility in (1) does not depend on  $\xi$ . Within this context, especially if (1) is estimated by the standard approach, it is crucial to quantify the dependence between the demand parameter  $D$  and various  $IM$  definitions to implicitly determine whether or not fragilities, defined as function of the commonly used  $IMs$ , can provide useful information for PBEE of actual complex multi-degree of freedom (MDOF) linear and nonlinear structural systems. If the dependence between  $D$  and  $IM$  is strong, the fragility  $P_f(\xi)$  gives accurate information (Ciano et al. submitted; 2018). The opposite holds when the dependence between  $D$  and  $IM$  is weak. Several statistical tools can be used to investigate the dependence between the random variables  $D$  and  $IM$ , which includes correlation coefficients,

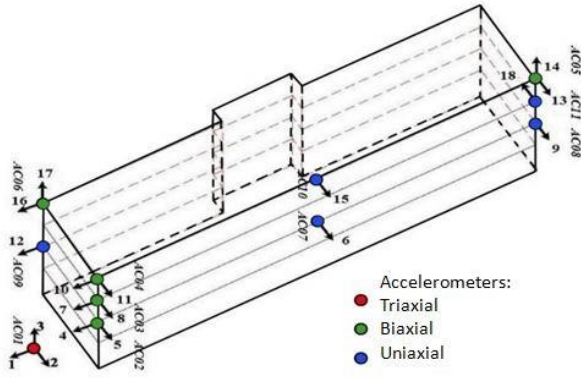


Figure 1. Scheme of the monitoring system of the Norcia school building.

copula models and multivariate extreme value theory (Grigoriu 2016). In this work an example of scatter plots of  $D$  and  $IM$  are used to give information on their correlation coefficients.

## 2.2 Demand parameters

Let  $X(t)$  be the response vector-valued process of an arbitrary MDOF structural system to the ground acceleration  $A(t)$ . The demand parameter is defined as

$$D = \max_{0 \leq t \leq \tau} |h(X(t))| \quad (2)$$

where  $\tau$  is the time length of  $A(t)$ , while  $h(\cdot)$  is a function mapping the response  $X(t)$  into the system demand parameter of interest, e.g. max inter-story displacement. In this work the maximum absolute displacement of each degree of freedom,  $D_d$ , is considered as demand parameter in the fragility analysis.

## 2.3 Intensity Measures (IMs)

The  $IMs$  used in PBEE to scale seismic acceleration ground motion are divided into three broad categories: (i) non-structures-specific scalar  $IMs$ ; (ii) structures-specific scalar  $IMs$ ; (iii) vector-valued  $IMs$ . A complete classification of the most known  $IMs$  in literature is reported in (Ebrahimian et al. 2015). In this paper the following  $IMs$  are considered to estimate the fragilities by standard approach

$$IM_1 = PGA \quad (3)$$

$$IM_2 = S_a(T_1, \zeta_1) \quad (4)$$

$$IM_3 = S_a(T_3, \zeta_3) \quad (5)$$

$$IM_4 = I_h \quad (6)$$

$$IM_5 = S^*(T_1, \zeta_1, C, \alpha) \quad (7)$$

where  $T_1$  and  $T_3$  are the first and third natural periods of the MDOF structural system, respectively, with associated damping ratios  $\zeta_1$  and  $\zeta_3$ ;  $I_h$  is the Housner intensity (Housner 1952);  $S^*(T_1, \zeta_1, C, \alpha)$  is the multi-parameter scalar  $IM$  functional of  $IM_2$  (Cordova et al. 2000) with  $C=2$  and  $\alpha=0.5$ . In this work  $T_1$  is selected since it is the fundamental period of the structure in  $x$ -direction (Figure 2) as is customary in the literature (Ebrahimian et al. 2015);  $T_3$  is also considered because it assumes a large participating mass in the  $y$ -direction (Figure 2). Details of the structure modal parameters can be found in (Ciano et al. 2018).

## 3 CASE STUDY NUMERICAL MODEL ANALYSIS

The school in Norcia is used as benchmarks for many studies in Italy. Particular interest comes from the continuous monitoring system, powered by Italian National Seismic Observatory, at several locations in the building (Figure 1). The structural system consists of a reinforced concrete frame (RCF) on four floors with a dissipative bracing system, Buckling-Restrained Axial Dampers (BRAD), and inverse beams foundation. Details on the school building are reported in (Ciano et al. 2018). The RCF and foundation are modeled with classical beam elements, while for the BRAD elements the constitutive law (Wen 1976) is used. Experimental data by the monitoring system were used to calibrate the FE model.

IDA analyses are performed to evaluate the displacement demand parameter  $D_d$  for each compatible acceleration time histories, while in

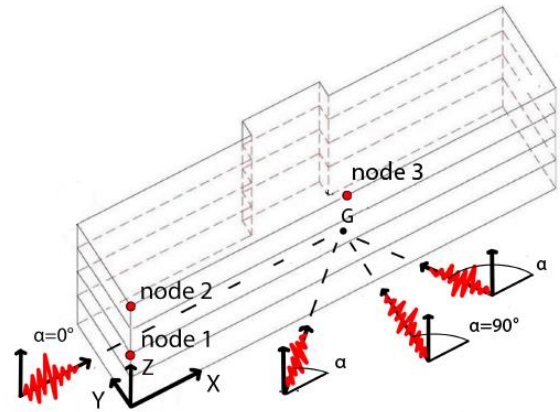


Figure 2. Seismic directions used in the analyses and reference node locations.

system degree of freedom when the model is subjected to different samples of  $A(t)$  in  $x$  or  $y$  global-directions (Figure 2). The first results for linear and nonlinear structural analyses are reported in (Ciano et al. submitted) where spectra-compatible acceleration time histories were used for the fragilities estimation. In this work linear IDAs are performed to access fragilities by both standard and alternative methods when the model is subjected to simulated stochastic process and stochastic process by SAM of actual school site, respectively.

The strong event recorded in Norcia on October 30<sup>th</sup>, 2016 is used to calibrate the stochastic non-stationary process  $A(t)$ .

## 4 SEISMIC GROUND ACCELERATION STOCHASTIC PROCESSES

### 4.1 Non-stationary model #1

Let  $Z(t)$  be a non-stationary stochastic process described by (Grigoriu et al. 1988)

$$Z(t) = c(t)Y(\varphi(t)) \quad (8)$$

where  $Y(t)$  is a real-valued zero-mean wide sense stationary process with variance  $\sigma_Y^2$  and one-sided spectral density  $G_Y(\omega)$ ,  $c(t)$  and  $\varphi(t)$  are amplitude and frequency modulation function, respectively. The time-dependent variance of  $Z(t)$  has expression

$$\sigma_Z^2(t) = c^2(t)\sigma_Y^2 \quad (9)$$

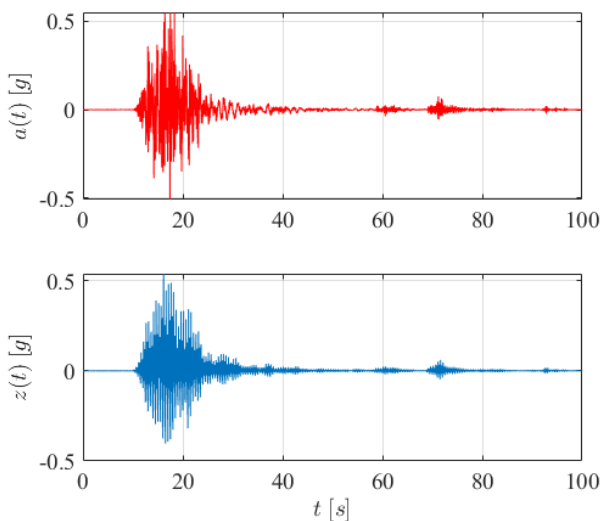


Figure 3. Acceleration time history  $AC01-1$  (Figure 1) recorded in Norcia on October 30<sup>th</sup>, 2016 (top); simulated sample of the non-stationary process  $Z(t)$  in (8) (bottom).

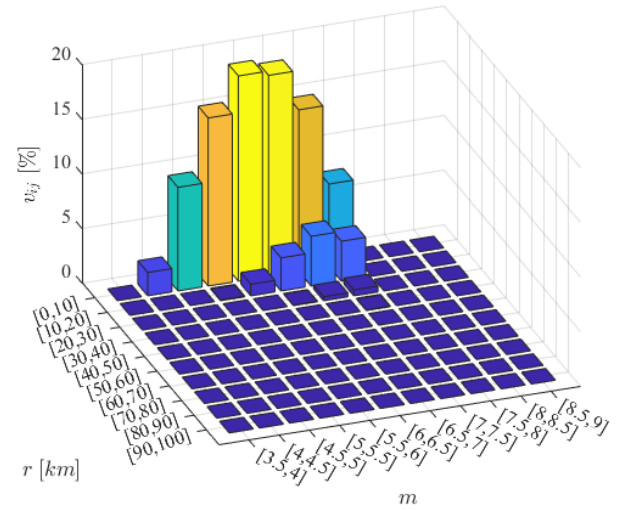


Figure 4. Seismic activity matrix of the Norcia school building site.

while the one-sided spectral density can be described as

$$G_Z(t, \omega) = c^2(t)G_Y(\omega) \quad (10)$$

in order to define the process in (8) as a uniformly modulated process.

The  $AC01$  (Figure 1) experimental components of the October 30<sup>th</sup>, 2016 event ( $m = 6.5$  and  $r = 5$  km) with  $PGA = 0.55$  g are used to calibrate the model (8) in order to generate  $n_s$  independent samples of  $z_i(t)$ ,  $i = 1, \dots, n_s$ , of the process  $Z(t)$ .

Figure 3 shows the experimental record (top panel) in the building  $x$ -direction (Figure 2), i.e.  $AC01-1$  in Figure 1 together with one sample of simulated acceleration time history using the model in (8) (bottom panel).

### 4.2 Non-stationary model #2

Let  $W(t)$  be a non-stationary empirically calibrated stochastic process. Samples of  $W(t)$  can be generated by the approach proposed in (Yamamoto and Baker 2013) using the inverse wavelet packet transform (WPT)

$$w(t) = \sum_{i=1}^{2^j} \sum_{k=1}^{2^{N-j}} b_{j,k}^i \gamma_{j,k}^i(t) \quad (11)$$

where  $b_{j,k}^i$  is the  $i$ -th set of wavelet packet coefficients at the  $j$ -th scale parameter and  $k$ -th translation parameter,  $\gamma_{j,k}^i$  is the wavelet packet function, and  $2^N$  denotes the steps number in the time series. The wavelet packet coefficients are evaluated on past earthquake scenario as in (Yamamoto and Baker 2013). The wavelet packet coefficients need to be evaluated as a function of the scenario parameters, such as site feature and

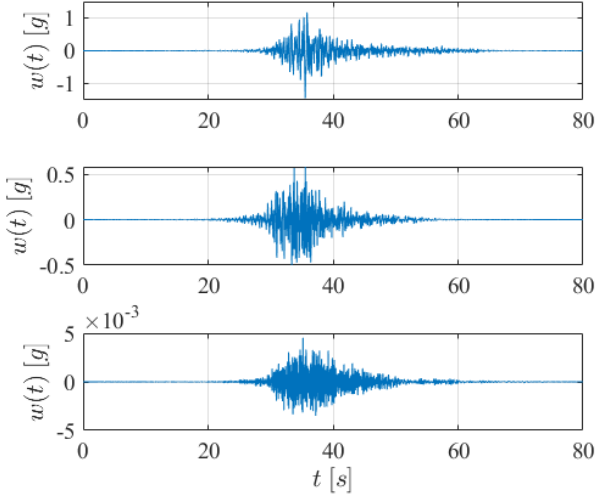


Figure 5. Samples  $w(t)$  of model #2 stochastic process based on the site seismic activity matrix in Figure 4:  $m = 7.5$  and  $r = 10$  km (top);  $m = 6.5$  and  $r = 5$  km (middle);  $m = 4.5$  and  $r = 50$  km (bottom).

magnitude, to generate a ground motion representing a particular scenario. To predict a future earthquake scenario a two-stage regression analysis is performed based on  $m$ ,  $r$  and the average shear-wave velocity within 30 m depth  $V_{S30}$  as predictor variables.

Figure 4 shows the SAM of the Norcia school building site given by the Italian National Institute of Geophysics and Volcanology, i.e. the probability  $v_{ij}$  that an earthquake occurs at site for a couple of  $(m_i, r_j)$ . The disaggregation plot (Figure 4) is defined as the 2% probability of excess in 50 years with 84<sup>th</sup> percentile. Different  $n_s$  samples  $w_i(t)$ ,  $i = 1, \dots, n_s$ , of  $W(t)$  are generated using Equation (11) and the site scenario parameters given by the SAM in Figure 4 for  $V_{S30}=678$  m/s.

Figure 5 shows three samples of  $w(t)$  for the scenarios:  $(m = 7.5, r = 10$  km),  $(m = 6.5, r = 5$  km) and  $(m = 4.5, r = 50$  km) in the top, middle and bottom panel, respectively. The sample  $w(t)$  in the middle panel has PGA = 0.58 g.

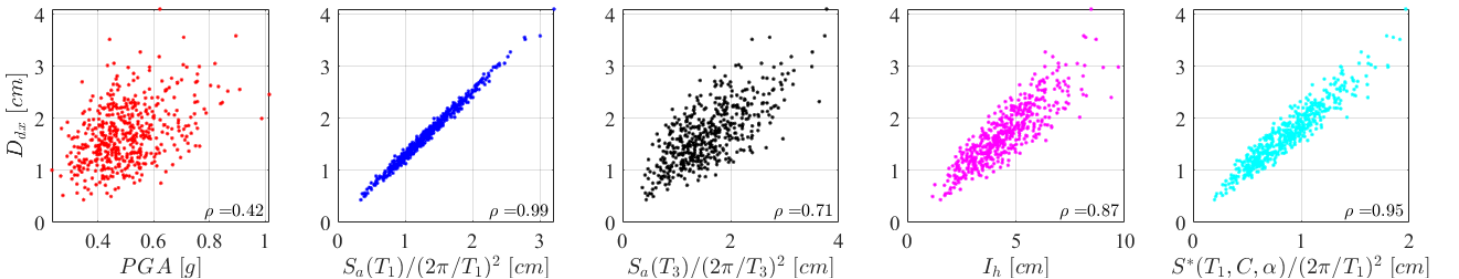


Figure 7. Scatter plots of  $n_s = 500$  samples of  $(PGA, D_{dx})$ ,  $(S_a(T_1)/(2\pi/T_1)^2, D_{dx})$ ,  $(S_a(T_3)/(2\pi/T_3)^2, D_{dx})$ ,  $(I_h, D_{dx})$ ,  $(S^*(T_1, C, \alpha)/(2\pi/T_1)^2, D_{dx})$ ,  $\alpha=0^\circ$ , at node #3 – linear analysis.

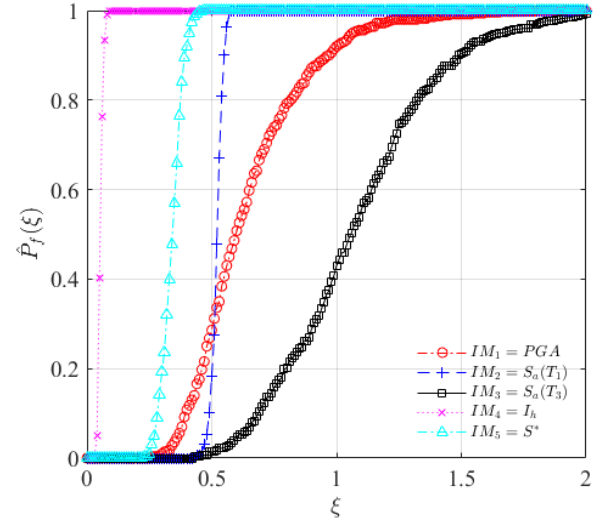


Figure 6. Fragilities against intensity level  $\xi$  for different definitions of  $IMs$  at node #3 with  $\alpha=0^\circ$ , displacements  $D_{dx}$  for limit state  $\bar{D}_{dx} = 2$  cm – linear analysis.

## 5 FRAGILITIES ESTIMATION

### 5.1 Standard approach

The seismic fragility analysis, as also recommended by FEMA, is commonly based on a four-steps algorithm consisting of scaling seismic accelerograms by a reference  $IM$ :

1. selection of a finite set of intensity measures  $\{\zeta_k\}$ ,  $k=1, \dots, N$ ;
2. generation of  $n_s = 500$  samples of  $A(t) = Z(t)$ , i.e.  $a_i(t) = z_i(t)$ ,  $i = 1, \dots, n_s$ ;
3. for each of the values  $\{\zeta_k\}$  scale the  $n_s$  acceleration records in order to have the intensity level  $IM = \zeta_k$ ,  $\zeta_k > 0$ ;
4. for each of the values  $\{\zeta_k\}$  estimate fragility as

$$\hat{P}_f(\zeta_k) = \sum_{j=1}^{n_s} 1(d_{k,j} \in I) / n_s \quad (12)$$

where  $1(\cdot)$  is the indicator function and  $d_{k,j}$ ,  $j=1, \dots, n_s$ , are samples of the demand parameters computed for each intensity level  $\{\zeta_k\}$  by IDA.

Figure 6 reports fragility curves estimated by four-steps algorithm described above, using different  $IM$  definitions ( $IM_l$ ,  $l=1,\dots,5$ ) (3)-(7)) and linear IDA analyses for the demand parameter  $D_{dx}$  (i.e. the maximum absolute displacement in  $x$ -direction) at node #3, assuming earthquake direction  $\alpha=0^\circ$  (Figure 2) and limit state  $\bar{D}_{dx} = 2$  cm. Results show the fragilities variability with the  $IM$  used in the analysis. The role of  $IMs$  on the accuracy of seismic fragilities when using this standard procedure was widely discussed in (Ciano et al. submitted) for the same case study. The ability of the standard approach to provide accurate fragility estimation can be evaluated investigating on the dependence between  $D_{dx}$  and the various  $IMs$  (Grigoriu 2016). Figure 7 shows scatter plots of  $n_s=500$  samples of the demand parameter  $D_{dx}$ , computed at node #3 with seismic direction  $\alpha=0^\circ$ , against the intensity measures  $IM_l$ ,  $l=1,\dots,5$ , one for each panel from left to right, respectively, together with the estimated correlation coefficient. Damping ratio is assumed to be  $\zeta_1 = \zeta_3 = \zeta = 5\%$  for  $IM_2, IM_3, IM_5$ .

The results presented in Figure 7 demonstrated that  $IM_2$  (second panel from left) is the best candidate to provide an accurate fragility curve for the selected demand parameter since the conditional variable  $D_{dx}|IM_2$  has small variance (i.e.  $D_{dx}$  and  $IM_2$  are correlated), while, in this case,  $IM_1$  (left panel), commonly used in PBEE, represents an unsatisfactory intensity measure since the low correlation coefficient between  $D_{dx}$  and  $IM_1$  will determine a fragility, which provides poor information on the seismic performance. The results has not general validity since it was demonstrated that  $IMs$  can be both strongly and weakly correlated with the demand parameter depending on the selected structural response of interest and the earthquake direction (Ciano et al. submitted).

## 5.2 Alternative approach

It is possible to estimate fragilities using virtual acceleration time series according to the model in Equation (13). The following two-steps algorithm can be used:

1. generation  $n_s = 500$  samples of  $A(t) = W(t)$ , i.e.  $a_i(t) = w_i(t)$ ,  $i = 1,\dots,n_s$ , for each couple  $(m, r)$  by SAM (Figure 4);
2. for each couple  $(m, r)$  estimate fragility as

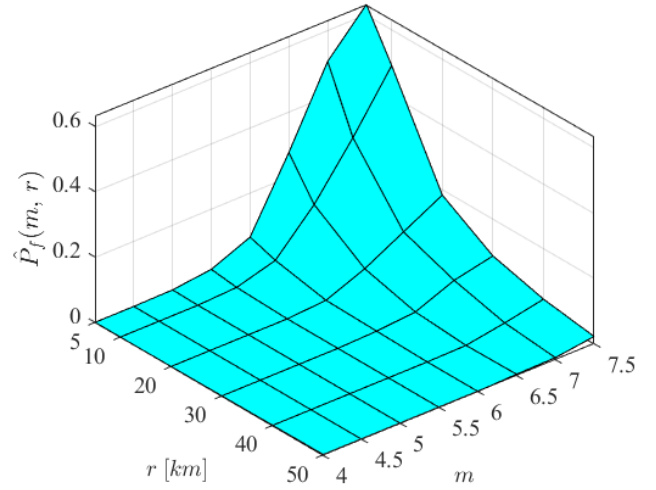


Figure 8. Fragility surface against couple  $(m, r)$  at node #3 with  $\alpha=0^\circ$ , displacements  $D_{dx}$  for limit state  $\bar{D}_{dx} = 2$  cm – linear analysis.

$$\hat{P}_f(m, r) = \sum_{j=1}^{n_s} 1(d_{k,j} \in I) / n_s \quad (14)$$

where  $1(\cdot)$  is the indicator function and  $d_{k,j}$ ,  $j=1,\dots, n_s$ , are samples of the demand parameters computed for each couple  $(m, r)$  by IDA. Equation (14) provides a fragility surface giving the probability that structural response of a system overcomes specified limit states for given magnitude  $m$  and distance site-to-source  $r$  (Kafali and Grigoriu 2007). Given the parameters  $(m, r)$  the probability law of the seismic ground acceleration is defined completely, and the inconvenience of scaling procedures does not occur (Grigoriu 2010).

Figure 8 reports the fragility surface computed by linear IDA for the demand parameter  $D_{dx}$ , limit state  $\bar{D}_{dx} = 2$  cm, at node #3 for earthquake direction  $\alpha=0^\circ$  (Figure 2).

It is worth noting that if one uses the parameters  $m = 6.5$  and  $r = 5$  km, i.e. the conditions happened on October 30<sup>th</sup>, 2016 at the school site, the estimated  $P_f$  is about 0.3. The same value can be obtained from the fragility curve by  $IM_2$  in Figure 6 for the intensity level  $\zeta = 0.5$ .

The fragility surface that uses SAM can be also obtained by crossing theory rather than with a raw Monte Carlo approach in order to provides accurate results with a lower computational cost (Kafali and Grigoriu 2007).

## 6 CONCLUSION

In performance-based earthquake engineering the seismic fragilities are commonly estimated by standard approach based on scaling the seismic accelerograms with a reference intensity measure ( $IM$ ). The shortcomings of this method are: (i) the scaled seismic accelerograms do not describe accurately the probability law of the unscaled records; (ii) a strong dependence is required between the demand parameter  $D$  of the structural system, on which the fragility analysis is based, and the  $IM$  used for scaling, in order to have accurate fragilities. The standard approach provides limited if any information on the seismic performance of the structural system for weak dependence between  $D$  and  $IM$ , and scaling seismic ground-accelerations is not recommended.

An alternative approach to estimate seismic fragilities was recently proposed by the third author, which is based on the site seismic activity matrix and is able to generate non-stationary seismic accelerograms depending on the earthquake moment magnitude and the source-to-site distance. This method gives seismic ground acceleration for different earthquake levels without using the scaling procedure typical of the standard approach. In this paper fragility analysis based on linear incremental dynamic analysis was performed using the two described approaches on an actual complex multi-degree of freedom structural system, a school building in Norcia, Italy. The numerical structural model was calibrated using experimental data obtained by the Italian National Seismic Observatory. The estimated fragility curves and surface demonstrated the high variability of the results depending on the approach used and on the selected intensity measure. These results should be seriously taken into account in Performance-Based Earthquake Engineering (PBEE) when estimating structural performance by fragility analysis in order to avoid unreliable designs.

## ACKNOWLEDGEMENTS

The work of the third author reported in this paper has been partially supported by the National Science Foundation under grant CMMI-1639669. This support is gratefully acknowledged.

## REFERENCES

- Baker, J. W., 2010. Conditional mean spectrum: Tool for ground-motion selection. *Journal of Structural Engineering*, **137**(3), 322–331.
- Ciano, M., Giofrè, M., Grigoriu, M., submitted. The role of intensity measures on the accuracy of seismic fragilities. *Submitted: Probabilistic Engineering Mechanics*.
- Ciano, M., Giofrè, M., Grigoriu, M., 2018. On the accuracy of seismic fragilities for actual non-linear MDOF systems. In: *Proceedings of the CSM8 Eighth Conference on Computational Stochastic Mechanics*. Paros.
- Cordova, P. P., Deierlein, G. G., Mehanny, S. S. F., Cornell, C. A., 2000. Development of a two-parameter seismic intensity measure and probabilistic assessment procedure. *The Second US-Japan Workshop on Performance-Based Earthquake Engineering Methodology for Reinforced Concrete Building Structures*, 187–206.
- Ebrahimian, H., Jalayer, F., Lucchini, A., Mollaioli, F., Manfredi, G., 2015. Preliminary ranking of alternative scalar and vector intensity measures of ground shaking. *Bulletin of Earthquake Engineering*, **13**(10), 2805–2840.
- FEMA P-58, 2012a. *Seismic Performance Assessment of Buildings: Vol. 1—Methodology*. FEMA P-58.
- Grigoriu, M., 2016. Do seismic intensity measures (IMs) measure up? *Probabilistic Engineering Mechanics*, **46**, 80–93.
- Grigoriu, M., 2010. To scale or not to scale seismic ground-acceleration records. *Journal of Engineering Mechanics*, **137**(4), 284–293.
- Grigoriu, M., Ruiz, S. E., Rosenblueth, E., 1988. The Mexico earthquake of September 19, 1985—Nonstationary models of seismic ground acceleration. *Earthquake Spectra*, **4**(3), 551–568.
- Housner, G. W., 1952. Spectrum intensities of strong-motion earthquakes. In: *Proc. Symposium on Earthquake and Blast Effects on Structures*, Pp. 20–36.
- Kafali, C., Grigoriu, M., 2007. Seismic fragility analysis: Application to simple linear and nonlinear systems. *Earthquake Engineering & Structural Dynamics*, **36**(13), 1885–1900.
- Kwong, N. S., Chopra, A. K., McGuire, R. K., 2015a. A framework for the evaluation of ground motion selection and modification procedures. *Earthquake Engineering & Structural Dynamics*, **44**(5), 795–815.
- Kwong, N. S., Chopra, A. K., McGuire, R. K., 2015b. A ground motion selection procedure for enforcing hazard consistency and estimating seismic demand hazard curves. *Earthquake Engineering & Structural Dynamics*, **44**(14), 2467–2487.
- Kwong, N. S., Chopra, A. K., McGuire, R. K., 2015c. Evaluation of ground motion selection and modification procedures using synthetic ground motions. *Earthquake Engineering & Structural Dynamics*, **44**(11), 1841–1861.
- Lopez Garcia, D., Soong, T. T., 2003. Sliding fragility of block-type non-structural components. Part 1: unrestrained components. *Earthquake Engineering &*

- Structural Dynamics*, **32**(1), 111–129.
- O’connor, J. M., Ellingwood, B. R., 1992. Site-dependent models of earthquake ground motion. *Earthquake Engineering & Structural Dynamics*, **21**(7), 573–589.
- Radu, A., 2017. A Framework for Earthquake Risk Engineering. *Procedia Engineering*, **199**, 3576–3581.
- Radu, A., Grigoriu, M., 2018. An earthquake-source-based metric for seismic fragility analysis. *Bulletin of Earthquake Engineering*, **16**(9), 3771–3789.
- Wen, Y. X., 1976. Method for random vibration of hysteretic systems. *Journal of the Engineering Mechanics Division*, **102**(2), 249–263.
- Yamamoto, Y., Baker, J. W., 2013. Stochastic model for earthquake ground motion using wavelet packets. *Bulletin of the Seismological Society of America*, **103**(6), 3044–3056.